On the Throughput Capacity Study for Aloha Mobile Ad Hoc Networks

Yin Chen, *Member, IEEE*, Yulong Shen, *Member, IEEE*, Jinxiao Zhu, Xiaohong Jiang, *Senior Member, IEEE*, and Hideyuki Tokuda, *Member, IEEE*

***Abstract*—Despite extensive efforts on exploring the asymptotic capacity bounds for mobile ad hoc networks (MANETs), the general exact capacity study of such networks remains a challenge. As one step to go further in this direction, this paper considers two classes of Aloha MANETs (A-MANETs) $\mathcal{N}_A$ and $\mathcal{N}_C$ that adopt an aggressive traffic-independent Aloha and the conventional traffic-dependent Aloha, respectively. We first define a notation of successful transmission probability (STP) in $\mathcal{N}_A$, and apply queuing theory analysis to derive a general formula for the capacity evaluation of $\mathcal{N}_A$. We also prove that $\mathcal{N}_C$ actually leads to the same throughput capacity as $\mathcal{N}_A$, indicating that the throughput capacity of $\mathcal{N}_C$ can be evaluated based on the STP of $\mathcal{N}_A$ as well. With the help of the capacity formula and stochastic geometry analysis on STP, we then derive closed-form expressions for the throughput capacity of an infinite A-MANET under the nearest neighbor/receiver transmission policies. Our further analysis reveals that although it is highly cumbersome to determine the exact throughput capacity expression for a finite A-MANET, it is possible to have an efficient and closed-form approximation to its throughput capacity. Finally, we explore the capacity maximization and provide extensive simulation/numerical results.**

***Index Terms*—Throughput Capacity, Mobile Ad Hoc Networks, Aloha, Queuing Theory, Stochastic Geometry.**

I. Introduction

SINCE the seminal work of Grossglauser and Tse [2], extensive research efforts have been devoted to the study of throughput capacity scaling laws in mobile ad hoc networks (MANETs) [3], which mainly focus on determining the asymptotic bounds for throughput capacity as a function of the number of network nodes n. It was demonstrated in [2] that a $\Theta(1)$ per-node throughput is achievable in a MANET with i.i.d. mobility model, indicating that a constant per-node throughput can be ensured even as n grows to infinity. Gamal et al. [4] demonstrated that the $\Theta(1)$ per-node throughput is also achievable when each node moves independently following a symmetric random walk on a $\sqrt{n} \times \sqrt{n}$ grid, where a $\Theta(n \log n)$ average package delay is incurred. Mammen and Shah proved in [5] that a similar capacity-delay tradeoff exists in a MANET on a unit sphere with a restricted mobility model, where each node moves along a randomly chosen orthodrome on the sphere. Wang et al. explored the scaling laws of capacity and delay of a MANET with multicast traffic in [6], [7] and further conducted a theoretical comparison between the unicast and multicast MANETs in [8], which shows that mobility weakens the distinction of capacity scaling laws between unicast and multicast. For a survey on the capacity scaling laws of MANETs, readers are referred to [9] and references therein.

While the scaling law results of a MANET help us to understand the general asymptotic trend of its throughput capacity as network size increases, the exact result for the throughput capacity of such a network is of more interest for network design and performance optimization. Recently, some preliminary results on the exact throughput capacity study of MANETs have been reported in the literature [10]–[13] (See Section II-A for a brief review). Although these works represent a significant step towards the exact throughput capacity study of MANETs, many important network scenarios have not been explored yet, so the general exact throughput capacity study for MANETs still remains a challenge. As one step to go further on the exact throughput capacity study for MANETs, this paper focuses on MANETs with Aloha MAC protocol (A-MANETs) [14]. Since Aloha protocol is simple yet efficient and can be easily implemented in a distributed way, A-MANETs represent a class of important and practical networks. Triggered by the work of Baccelli et al, the performance of A-MANETs has been extensively studied in the last decade [14]–[24] (See Section II-B for a brief review). Despite of these extensive research efforts, the throughput capacity of A-MANETs remains largely unknown. This is mainly due to the following challenges. The first one is the correlation between the transmission scheduling and traffic in A-MANETs. Such correlation leads to an interacting queueing system in A-MANETs, which is in general not analytically tractable [25]. The second one is the complex geometric calculation involved in the derivation for the probability of successful transmissions which are typically interfered by other (randomly distributed) concurrent transmissions. To address the above challenges, this paper proposes a novel theoretical framework for the exact throughput capacity study of A-MANETs. The main contributions are summarized as follows.

Manuscript received September 27, 2015; revised January 19, 2016; accepted January 29, 2016. Date of publication February 8, 2016; date of current version April 13, 2016. This work is partially supported by Japan JSPS Grant 15H02692, China NSFC Grants 61571352, 61373173, and U153620014. Part of this work was published in preliminary form [1]. The associate editor coordinating the review of this paper and approving it for publication was L. Badia.
(Corresponding authors: Yin Chen and Yulong Shen.)

Y. Chen is with the Graduate School of Media and Governance, Keio University. Fujisawa 252-0882, Japan (e-mail: yin@ht.sfc.keio.ac.jp).

Y. Shen is with the School of Computer Science and Technology, Xidian University, Xi'an, China (e-mail: ylshen@mail.xidian.edu.cn).

J. Zhu is with the Advanced ICT Research Institute, National Institute of Information and Communications Technology (NICT), Tokyo 184-8795, Japan (e-mail: zhu@nict.go.jp).

X. Jiang is with the School of Systems Information Science, Future University Hakodate, Hakodate 041-8655, Japan (e-mail: jiang@fun.ac.jp).

H. Tokuda is with the Faculty of Environment and Information Studies, Keio University. Fujisawa 252-0882, Japan (e-mail: hxt@ht.sfc.keio.ac.jp).
Digital Object Identifier 10.1109/TCOMM.2016.2527658

1) For the capacity study of A-MANETs, we considered in Section III two classes of A-MANETs $\mathcal{N}_A$ and $\mathcal{N}_C$, where $\mathcal{N}_A$ adopts a traffic-independent aggressive Aloha protocol (A-Aloha) and $\mathcal{N}_C$ adopts the traffic-dependent conventional Aloha protocol (C-Aloha). In Section IV, we applied queuing theory to derive a general formula for the capacity evaluation of $\mathcal{N}_A$ based on a notation of successful transmission probability (STP) in $\mathcal{N}_A$. We then proved that the $\mathcal{N}_C$ leads to the same throughput capacity as $\mathcal{N}_A$. This indicates that the throughput capacity of $\mathcal{N}_C$ can also be evaluated based on the STP of $\mathcal{N}_A$, so the challenging correlation issue between the transmission scheduling and traffic in the $\mathcal{N}_C$ capacity study is circumvented.
2) We then conducted stochastic geometry analysis in Section V on the STP of $\mathcal{N}_A$ under the typical nearest neighbor/receiver transmission policy and protocol interference model [26], and determined the limit of the STP as the number of network node tends to infinity. With the help of the capacity formula and the STP limit, we then succeeded in deriving the exact expression for the throughput capacity of the infinite A-MANETs.
3) Our capacity analysis of finite A-MANETs in Section VI revealed that although it is highly cumbersome (if not possible) to determine the exact expression for the throughput capacity of such a network, it is possible to have a very efficient and closed-form approximation to its throughput capacity, which is accurate up to an additive error vanishing to zero exponentially with the number of nodes. Optimization was also conducted to determine the optimal value of the Aloha transmission probability for capacity maximization. We conducted simulation/numerical study in Section VII to verify the developed capacity/delay results and to illustrate the impact of network parameters on network performance.

II. Related Work

A. Exact Throughput Capacity Study of MANETs

Some preliminary results on the exact throughput capacity study of MANETs have been reported in the literature. Neely and Modiano [10] explored the exact throughput capacity of a cell-partitioned MANET, where the network area is evenly divided into discrete cells and the node mobility, transmission scheduling and interference are all defined based on these cells. Also, it is assumed in [10] that each cell accommodates at most one transmitter per time slot and adjacent cells adopt orthogonal channels for interference mitigation. Following the model of [10], Urgaonkar and Neely further investigated the inherent relation between capacity and energy consumption in [11]. Inspired by the work of [10], Chen et al. [12] studied the intermittently connected sparse MANET with Poisson contact process and derived its throughput capacity based on the pair-wise contact rate therein. For the special Manhattan and ring networks, their exact throughput capacity results have been reported in [13]. It is notable that different from the above studies [10]–[13], this paper considers a more sophisticated MANET model with continuous network area and Aloha MAC protocol, where interference and related transmission collisions are carefully taken into account. Notice also that for the throughput capacity evaluation of the concerned MANET, we need to address the cumbersome interacting queues problem which is not involved in the studies [10]–[13]. Thus, the capacity evaluation methods developed in [10]–[13] cannot be directly applied to the throughput capacity study of the concerned MANET. This paper addresses the interacting queues problem by first introducing a traffic-independent aggressive Aloha (A-Aloha) and then proving that the A-Aloha actually leads to the same throughput capacity as the traffic-dependent conventional Aloha (C-Aloha), so the throughput capacity of C-Aloha MANET can be evaluated based on its counterpart A-Aloha MANET.

B. Performance Studies for A-MANETs

By now, lot of work has been devoted to the study of the spatial performance statistics in A-MANETs, where the locations of nodes are often modeled by a Poisson point process. The asymptotic packet propagation behavior of A-MANETs was investigated in [14]–[16], while their interference issue and related outage performance were explored in [17]–[19]. The authors of [20] took a game-theoretical approach to study the power control in A-MANETs, and [21], [22] conducted analysis on the local delay in A-MANETs, i.e., the time it takes a node to successfully transmit a packet in such networks. Recently, the security issue in A-MANETs was explored in [23], [24]. Distinguished from these studies on the spatial performance statistics in A-MANETs, this paper studies the throughput capacity, an end-to-end performance metric of A-MANETs. In particular, we consider an A-MANET where the nodes locations under the concerned mobility model actually follows a Binomial point process in each time slot, and develop a novel approximation approach for the efficient capacity evaluation of the network.

III. System Models and Definitions

A. Network Model

We consider a time-slotted network with a continuous square area. Without loss of generality, the network area is normalized to 1 for the convenience of discussion [2], [10]. Similar to the previous studies [26]–[28], the network is assumed to have torus boundaries. There are $n \geq 3$ mobile nodes in the network, and they randomly move according to a two dimensional i.i.d. mobility model [10], [29]. Under this mobility model, each node independently and uniformly selects a point from the network area at the beginning of each time slot and then stays at it during the time slot, so in each time slot the location of each node is i.i.d. and uniformly distributed over the network area, and between time slots the distributions of nodes locations are independent. We adopt the models of torus network and i.i.d. mobility here mainly due to the following reasons. First, the mathematical tractability of these models allows us to gain important insights into the structure of throughput capacity analysis. Second, the analysis under the i.i.d. model provides a meaningful theoretical performance result in the limit of infinite mobility. Third, it follows from Corollary 5 of [30] that the results obtained with the i.i.d. model also provide a good estimation of those obtained with more realistic mobility models (like the random walk and random direction), as it will be further validated in Section VII.

B. Communication Model

A half-duplex medium is shared by all the nodes for data communication. The communication model consists of transmitter selection, receiver selection and criteria of correct reception. The following two slotted Aloha protocols are considered in this paper for transmitter selection:

Aggressive Aloha Protocol (A-Aloha) [25]: Under the A-Aloha protocol, in each time slot a node will become a transmitter with probability p or keep silent as a potential receiver with probability $1-p$ regardless of whether it gets packet(s) to transmit from routing layer. If a node does not get any packet to transmit from routing layer, it still conducts a "dummy-transmission" that causes nothing but interference to other concurrent transmissions.

Conventional Aloha Protocol (C-Aloha): Under the C-Aloha protocol, in each time slot a node will become a transmitter with probability p or keep silent as a potential receiver with probability $1-p$ given that it gets packet(s) to transmit from routing layer. If a node does not get any packet to transmit from routing layer, it will also keep silent as a potential receiver. For the convenience of discussion, we will use $\mathcal{N}_A$ and $\mathcal{N}_C$ hereafter to denote the A-MANET with the A-Aloha and that with the C-Aloha, respectively. It is considered that the $\mathcal{N}_A$ and $\mathcal{N}_C$ are only different in the underlying Aloha protocols and the remaining system models are identical.

Previous studies indicate that local transmission provides a better throughput performance than long-distance transmission schemes [2], [31], so we consider the following two local transmission schemes for receiver selection [22]: **Nearest Neighbor Transmission (NNT)**: Under NNT, the intended receiver of a transmitter is the node closest to the transmitter among all other nodes. **Nearest Receiver Transmission (NRT)**: Under NRT, the intended receiver of a transmitter is the silent node closest to the transmitter among all other nodes. We adopt the protocol model introduced in [26] to decide if a transmission between a transmitter and its intended receiver is correctly received. Under the protocol model, the transmission from transmitter i to receiver j is correctly received iff (if and only if) the following inequality holds for all simultaneously transmitting node l other than i,

$$d_{lj} \geq (1+\Delta)d_{ij}, \tag{1}$$

where d_{lj} denotes the Euclidean distance between nodes l and j, and $\Delta > 0$ is a guard interval. The disc area centered at receiver j with radius $(1+\Delta)d_{ij}$ models a guard zone to prevent the transmission from being corrupted by interference. During a transmission, the total amount of data that can be transmitted is fixed and normalized to one packet.

C. Traffic Model

For traffic model, we consider that there are n unicast traffic flows in the network, and each node is the source of one traffic flow and also the destination of another traffic flow. Denoting $\varphi(i)$ the destination node of the traffic flow originated from node i, the source-destination pairs are matched in a way that the sequence $(\varphi(1), \varphi(2), \ldots, \varphi(n))$ is just a derangement of the set of nodes $\{1, 2, \ldots n\}$.[1] Two typical examples of this traffic model are $\varphi(1) = 2, \varphi(2) = 3, \ldots, \varphi(n) = 1$ and $\varphi(1) = 2, \varphi(2) = 1, \ldots, \varphi(n-1) = n, \varphi(n) = n-1$ [10]. We assume that the packet arrival process at each node is an i.i.d. Bernoulli process with rate λ packets/slot, so that with probability λ, a single packet arrives at the node at the beginning of each time slot. To simplify analysis, we assume that there is no constraint on packet lifetime and the node buffer size is sufficiently large so that packet loss due to buffer overflow will never occur.

D. Performance Metrics

End-to-end delay: For a tagged packet, its *end-to-end* delay is a random variable defined as the time elapsed between the time slot when the packet arrives at its source node and the time slot when it reaches its destination node. We use $\mathbb{E}\{D\}$ and $\mathbb{E}\{D_i\}$ to denote the expected end-to-end delay of the network and that of flow i, respectively. Based on temporal ergodicity, $\mathbb{E}\{D_i\}$ is given as $\mathbb{E}\{D_i\} = \lim_{k\to\infty} \frac{1}{k}\sum_{m=1}^{k} D_{i,m}$, where $D_{i,m}$ is the end-to-end delay of packet m of flow i. Since the traffic is symmetric, we have $\mathbb{E}\{D\} = \mathbb{E}\{D_1\} = \ldots = \mathbb{E}\{D_n\}$.

Throughput: The *throughput* of a traffic flow is defined as the time average of number of packets that can be delivered from its source to destination.

Throughput capacity and Maximum capacity: For an A-MANET with Aloha parameter p, the network is called *stable* under packet arrival rate λ (packets/slot) to each node if there exists a corresponding packet routing algorithm to ensure that as time evolves the queue length of each node does not grow to infinity (and thus the expected end-to-end delay is bounded). The *throughput capacity* μ of the A-MANET is then defined as the maximum value of λ that the network can stably support where the optimization is over all possible routing algorithms [10], [30] and the *maximum capacity* μ^* of the network is defined as the maximum value of throughput capacity μ optimized over parameter p, i.e., $\mu^* = \max_{p\in(0,1)} \mu$.

IV. General Throughput Capacity Analysis

In this section, we firstly study the A-MANET $\mathcal{N}_A$. In particular, we define a notion of successful transmission probability in $\mathcal{N}_A$ and present first a theorem to show how the throughput capacity of $\mathcal{N}_A$ can be evaluated based on this notion and then the necessary and sufficient stability conditions to prove the theorem. Secondly, we study the A-MANET $\mathcal{N}_C$. We prove that the same necessary and sufficient conditions of the network

[1] A derangement is a permutation that has no fixed point, i.e., $\varphi(i) \neq i$, $i = 1, 2, \ldots, n$.

stability of $\mathcal{N}_A$ actually also hold for the corresponding $\mathcal{N}_C$ and thus $\mathcal{N}_C$ has the same throughput capacity as $\mathcal{N}_A$.

A. Throughput Capacity Evaluation for $\mathcal{N}_A$

Successful transmission probability in $\mathcal{N}_A$ (STP): In the concerned A-MANETs, a node is called to conduct a *successful transmission* in a time slot iff (if and only if): In this time slot, 1) the node becomes a transmitter; 2) the intended receiver of the node is silent; 3) the transmission from the transmitter can be correctly received by the receiver. Notice that in the A-MANET $\mathcal{N}_A$, the probability that a node conducts a successful transmission is identical for each node and each time slot due to the i.i.d. mobility model and the communication model. Therefore, the *successful transmission probability in* $\mathcal{N}_A$, denoted by P_S, is defined as the probability that a node can conduct a successful transmission in a time slot. Notice that in the A-MANET $\mathcal{N}_A$, the probability that a node conducts a transmission is independent of the traffic. Notice also that the P_S is not conditioned on a transmission attempt occurring. In the analysis hereafter we will call P_S the STP for the convenience of discussion. In this section, the STP is taken as a given parameter, but its value and relation with system parameters (transmission probability p, guard interval Δ) will be investigated in Section V.

Theorem 1: Consider an A-MANET $\mathcal{N}_A$ where there are n mobile nodes and the A-Aloha is adopted. If we use P_S to denote its STP, then the throughput capacity of $\mathcal{N}_A$ is given by

$$\mu = \frac{n}{2(n-1)} P_S. \tag{2}$$

The proof of Theorem 1 involves proving that $\lambda \leq \mu$ is necessary and $\lambda < \mu$ is sufficient for ensuring network stability in $\mathcal{N}_A$. Following the technique of [10], we prove the necessity and sufficiency in Sections IV-A1 and IV-A2, respectively, by showing that μ is an upper-bound on the throughput of any routing algorithm and Algorithm 1 stabilizes the network for any $\lambda < \mu$.

1) Proof of Necessity:

Lemma 1: (**Necessity**) In a stable A-MANET $\mathcal{N}_A$ with n mobile nodes and STP P_S, its throughput under any routing algorithm is upper-bounded by

$$\mu = \frac{n}{2(n-1)} P_S. \tag{3}$$

Proof: At first, we note that if $\mathcal{N}_A$ is stable, the sum of arrival rates must be less than or equal to the sum of throughputs of all n traffic flows. Consider an arbitrary routing algorithm that can stablize $\mathcal{N}_A$ under arrival rate λ. We use $X_h(T)$ to denote the total number of packets transferred through h hops from their sources to destinations in time interval $[0, T]$. Formally, it is required that for any given $\epsilon > 0$, there must exist an arbitrarily large T such that

$$\lambda n - \epsilon \leq \frac{1}{T} \sum_{h=1}^{\infty} X_h(T), \tag{4}$$

where λ is the packet arrival rate at each node. Notice that in the time interval $[0, T]$, the total number of transferred packets is at least $\sum_{h=1}^{\infty} h X_h(T)$, which must be upper bounded by the total number of successful transmissions $Y(T)$ in this time interval since it costs at least one successful transmission to transfer a packet from one node to another. Thus, we have

$$\sum_{h=1}^{\infty} h X_h(T) \leq Y(T). \tag{5}$$

From (4) and (5), we have

$$\frac{1}{T} Y(T) \geq \frac{1}{T} X_1(T) + \frac{2}{T} \sum_{h=2}^{\infty} X_h(T) \geq \frac{1}{T} X_1(T) + 2\left[(\lambda n - \epsilon) - \frac{1}{T} X_1(T)\right], \tag{6}$$

$$\lambda \leq \frac{1}{2n}\left[\frac{1}{T} Y(T) + \frac{1}{T} X_1(T) + 2\epsilon\right]. \tag{7}$$

Based on the property of the i.i.d. mobility, we can see that for each node, its expected number of successful transmissions in one time slot is just equal to STP P_S. Thus, by applying the law of large numbers, we have that as $T \to \infty$

$$\frac{1}{T} Y(T) \xrightarrow{\text{a.s.}} n P_S. \tag{8}$$

Since a packet can be transferred from its source to its destination through single hop only when the source can conduct a successful transmission directly to the destination, $X_1(T)$ is upper bounded by the total number of successful transmissions $Y_{sd}(T)$ between all source-destination pairs in time interval $[0, T]$. Also, based on the i.i.d. mobility, a transmitter selects a node from the others with probability $\frac{1}{n-1}$. Since each node has only one source node according to the derangement traffic model, the expected number of successful transmissions directly from one node to its destination node in one time slot is equal to $\frac{1}{n-1} P_S$. Thus, as $T \to \infty$

$$\frac{1}{T} Y_{sd}(T) \xrightarrow{\text{a.s.}} \frac{n}{n-1} P_S. \tag{9}$$

Substituting (8) and (9) into (7), we have

$$\lambda \leq \frac{n}{2(n-1)} P_S + \frac{\epsilon}{n}, \text{ as } T \to \infty. \tag{10}$$

Since ϵ can be arbitrarily small, the result then follows. ∎

2) Proof of Sufficiency: In this section, we will prove that the upper bound μ in (3) is just the throughput capacity of $\mathcal{N}_A$. The basic idea of our proof is to show that for any $\lambda < \mu$, the delay $\mathbb{E}\{D\}$ under Algorithm 1 is bounded and thus the network stability is ensured.

Lemma 2: (**Sufficiency**) In the A-MANET $\mathcal{N}_A$ with n mobile nodes and STP P_S, if the packet arrival process at each node is an i.i.d. Bernoulli stream with rate $\lambda < \mu$ and the Algorithm 1 is adopted for packet routing, the expected end-to-end packet delay of the network $\mathbb{E}\{D\}$ is

$$\mathbb{E}\{D\} = \frac{n - \lambda - 1}{\mu - \lambda} = \frac{n - \rho\mu - 1}{(1-\rho)\mu}, \rho = \lambda/\mu. \tag{11}$$

Proof: At first, we present Algorithm 1 as follows:

Algorithm 1: Consider a transmitter Tx and its receiver Rx in the current time slot. If Rx is the destination node of Tx: Tx conducts *source-to-destination* transmission to Rx; otherwise Tx flips an unbiased coin. If it is the head, Tx conducts *source-to-relay* transmission to Rx; otherwise Tx conducts *relay-to-destination* transmission to Rx. If the transmission is successfully received at Rx[2], Tx will remove the transmitted packet from buffer; otherwise Tx still keeps the packet.

Queuing Structure: To support the operation of Algorithm 1, each node maintains one source queue to store locally generated packets and $n-2$ relay queues to store packets of other flows (one queue per flow). All the queues follow the first-in-first-out discipline.

Source-to-destination: If Tx has packet(s) in its local queue, then Tx sends the head-of-line packet of the queue to Rx. Otherwise, Tx sends a null-packet to Rx.

Source-to-relay: If Tx has packet(s) in its local queue, then Tx sends the head-of-line packet of the queue to Rx. Otherwise, Tx sends a null-packet to Rx.

Relay-to-destination: If Tx has packet(s) in the relay queue destined for Rx, then Tx sends the head-of-line packet of the queue to Rx. Otherwise, Tx sends a null-packet to Rx.

Under Algorithm 1, if a transmitter's corresponding local/relay queue is empty, the transmitter will send a null-packet to the receiver. This null-packet will be treated as a normal packet by the MAC layers of the transmitter and receiver, but will be dropped (if correctly received) by the routing layer of the receiver and thus the transmission of a null-packet will place no impact on the queueing process of the receiver.

Recall that in $\mathcal{N}_A$, the probability that a node conducts a successful transmission in a time slot is just equal to P_S. We use P_{sd}, P_{sr} and P_{rd} to denote the probabilities that a node can conduct a successful transmission in a time slot and according to Algorithm 1 the transmission will be scheduled as a source-to-destination, source-to-relay or relay-to-destination transmission, respectively. Based on the properties of the i.i.d. mobility, communication model and derangement traffic, we can see that for one node that can conduct a successful transmission in a time slot, with probability $1/(n-1)$ the receiver of this node is just its destination node and thus this transmission will be scheduled as a source-to-destination transmission under Algorithm 1. Therefore, the probability P_{sd} is determined as $P_{sd} = \frac{1}{n-1} P_S$. Similarly, for a node that can conduct a successful transmission in a time slot, with probability $\frac{n-2}{2(n-1)}$ the transmission will be scheduled as a source-to-relay or relay-to-destination transmission according to Algorithm 1. Thus, we can see that the probabilities P_{sr} and P_{rd} are determined as $P_{sr} = P_{rd} = \frac{n-2}{2(n-1)} P_S$.

Notice that based on our system models, the queuing process of each flow has the following properties: i) the packet arrival process to each flow is an i.i.d. Bernoulli process with the same rate λ; ii) based on Algorithm 1, each flow is served equally without priority, so each flow experiences the same service process. Due to these properties, the queuing process of each flow is identically distributed. We focus on a flow i in the following analysis and study its expected delay $\mathbb{E}\{D_i\}$. With the help of P_{sd}, P_{sr} and P_{rd}, the packet routing process of flow i under Algorithm 1 is illustrated in Fig. 1, where the source node conducts a successful source-to-destination transmission with probability P_{sd} and conducts a successful source-to-relay transmission to one relay node with probability $\frac{P_{sr}}{n-2}$, and a relay node conducts a successful relay-to-destination transmission to the destination node with probability $\frac{P_{rd}}{n-2}$. We can see from Fig. 1 that the packet routing process of a flow involves a two-stage relay process if the packet is not directly transmitted to the destination. The first stage is the queuing process at the source node, while the second stage is the queuing process at one relay node.

[2]Any node other than Rx will discard this packet if it receives the packet in this time slot.

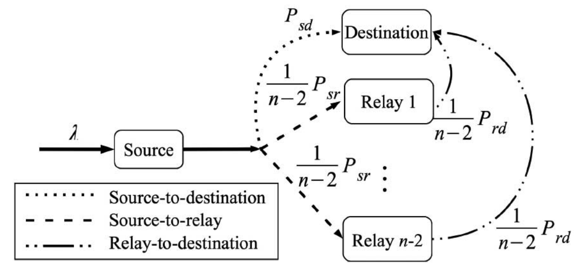

Fig. 1. The packet routing process of a single traffic flow under the Algorithm 1.

Firstly, for the source queue, its packet arrival rate is λ and its service rate is $P_{sd} + P_{sr} = \mu$. Denoting l the length of the source queue, its stationary distribution $\pi(l)$ is given by [32]

$$\pi(0) = \left(1 - \frac{\lambda}{\mu}\right)$$

$$\pi(l) = \left(1 - \frac{\lambda}{\mu}\right)\left(\frac{\lambda(1-\mu)}{\mu(1-\lambda)}\right)^l \left(\frac{1}{1-\mu}\right) \text{ for } l \geq 1. \quad (12)$$

Thus, the expected queue length $\mathbb{E}\{l\}$ at the source is $\mathbb{E}\{l\} = \sum_{l=1}^{\infty} l\pi(l) = \frac{\lambda^2-\lambda}{\lambda-\mu}$. Notice that the queue at the source is reversible, so its output is also a Bernoulli stream with rate λ [32].

Secondly, to analyze the queuing process at one of the $n-2$ relay nodes, we need to know the conditional probability that a packet is transmitted to this relay node given that it leaves its source. Using the definition of conditional probability, this probability can be determined as $\frac{P_{sr}}{(n-2)} \cdot \frac{1}{P_{sd}+P_{sr}} = \frac{1}{n}$, where $\frac{P_{sr}}{(n-2)}$ is the probability that the source conducts a successful source-to-relay transmission to the relay node, and $P_{sd} + P_{sr}$ is the probability that the source node conducts a successful source-to-destination or source-to-relay transmission. Based on the above conditional probability and the fact that the output from the source node is a Bernoulli stream with rate λ, we know that the packet arrival process to a relay node is a Bernoulli stream with rate $\lambda_r = \frac{\lambda}{n}$. Regarding the service rate μ_r of the relay queue, it is equal to the probability of successfully performing the relay-to-destination transmission with respect to a given destination, which is determined as $\mu_r = \frac{P_{rd}}{n-2} = \frac{P_S}{2(n-1)}$ according to the derangement traffic model. Denoting l_r the relay queue length, its stationary distribution $\pi_r(l_r)$ is

$$\pi_r(l_r) = \left(1 - \frac{\lambda_r}{\mu_r}\right)\left(\frac{\lambda_r}{\mu_r}\right)^{l_r}, \ l_r \geq 0. \quad (13)$$

Thus, the expected queue length $\mathbb{E}\{l_r\}$ at a relay node is $\mathbb{E}\{l_r\} = \sum_{l_r=1}^{\infty} l_r \pi_r(l_r) = \frac{\lambda_r}{\mu_r - \lambda_r}$. From Little's Theorem, the expected end-to-end delay $E\{D_i\}$ of any traffic flow i is evaluated as $\mathbb{E}\{D_i\} = [\mathbb{E}\{l\} + (n-2)\mathbb{E}\{l_r\}]/\lambda = \frac{n-\lambda-1}{\mu-\lambda}$, then (11) follows. ■

B. Throughput Capacity Evaluation for $\mathcal{N}_C$

In this section, we will prove that the necessary and sufficient conditions of the network stability developed in the above section for $\mathcal{N}_A$ actually also hold for $\mathcal{N}_C$ and thus the throughput capacity of $\mathcal{N}_C$ can be calculated based on the STP P_S of $\mathcal{N}_A$.

Theorem 2: Consider an A-MANET $\mathcal{N}_C$ where there are n mobile nodes and the C-Aloha is adopted. If we use P_S to denote the STP of the corresponding A-MANET $\mathcal{N}_A$ with n nodes and A-Aloha, then the throughput capacity of the $\mathcal{N}_C$ is given by

$$\mu = \frac{n}{2(n-1)} P_S. \tag{14}$$

Proof: The main idea is to show that the necessary and sufficient conditions developed in Lemmas 1 and 2 also hold for the $\mathcal{N}_C$, and thus the μ of (2) is also the throughput capacity of $\mathcal{N}_C$. Recall that the C-Aloha and A-Aloha are only different in that: when a node does not get any packet to transmit from the upper layer routing algorithm, the C-Aloha will make the node keep silent while the A-Aloha will still make the node conduct a dummy-transmission with probability p. Firstly, we know from Lemma 1 that for each $\lambda > \mu$, the $\mathcal{N}_A$ is unstable for any routing algorithm, indicating that the queue length in each node will grow to infinity and the probability that a transmitter conduct a dummy-transmission is zero. Since the dummy-transmission occurs with zero probability, the $\mathcal{N}_A$ and $\mathcal{N}_C$ are indistinguishable, indicating that the queue length in each node of $\mathcal{N}_C$ will also grow to infinity [25]. This observation implies that the $\mathcal{N}_C$ cannot be stabilized for any $\lambda > \mu$ and thus μ is also an upper bound on the throughput capacity of $\mathcal{N}_C$. Secondly, the upper bound μ can also be achieved by adopting Algorithm 1 in $\mathcal{N}_C$. This is because the Algorithm 1 always sends packets to the MAC layer (Algorithm 1 sends a null-packet if the corresponding queue is empty). Therefore, if the Algorithm 1 is employed, the A-Aloha and C-Aloha actually perform the same, implying that the Lemma 2 also holds for the $\mathcal{N}_C$. The theorem follows by summing up the above arguments. ■

Notice that Algorithm 1 generates null-packets, which place no impact on the queueing system but cause interference. To understand how Algorithm 1 can achieve the throughput capacity of the $\mathcal{N}_A$ and $\mathcal{N}_C$, we should notice that transmission of a null-packet under Algorithm 1 occurs only when the corresponding source/relay queue is empty, an event that becomes increasingly unlikely as input rate approaches the throughput capacity μ. In particular, if we let P_{null} denote the probability that a transmitter transmits a null-packet under the Algorithm 1, P_{null} corresponds to the probability that the source queue is empty when a source-to-destination or source-to-relay transmission is selected and the probability that the relay node queue is empty when a relay-to-destination transmission is selected. Based on (12) and (13), P_{null} can be determined as

$$\begin{aligned} P_{\text{null}} &= \frac{1}{n-1}\pi(0) + \frac{n-2}{2(n-1)}\pi(0) + \frac{n-2}{2(n-1)}\pi_r(0) \\ &= \left(1 - \frac{\lambda}{\mu}\right) \\ &= (1-\rho), \end{aligned} \tag{15}$$

which indicates clearly that as $\rho \to 1$, i.e., $\lambda \to \mu$, P_{null} vanishes to zero. Theorems 1 and 2 indicate that the only remaining issue in the throughput capacity calculation for $\mathcal{N}_A$ and $\mathcal{N}_C$ is to compute the STP P_S of $\mathcal{N}_A$, which will be addressed in Sections V and VI.

V. Throughput Capacity of Infinite Network

This section studies the infinite network scenario where the number of network nodes n grows to infinity. The exact expressions for the STP P_S of the infinite $\mathcal{N}_A$ network under the NNT and NRT will be derived, and then the exact expressions for the throughput capacity are obtained.

A. Modeling the STP P_S of $\mathcal{N}_A$

In this section, we evaluate the STP P_S of $\mathcal{N}_A$ under the NNT and NRT schemes, respectively. At first, we note that according to the definition of STP, when evaluating this probability, the node under consideration is randomly distributed over the network arena in the considered time slot and spatial averaging should be taken over the locations of all the other nodes. Due to the i.i.d. mobility and torus boundary considered in this paper, the distribution of the nodes' locations in each time slot is spatially stationary and ergodic, which implies that the STP in the time slot under consideration is just equal to the STP conditioned on that the node under consideration is located in an arbitrarily selected point (e.g., the center) of the network arena (Chapter 1.6 in [33] and Chapter 12 in [34]. Based on this property and for discussion convenience, we will assume in the following sections that the considered node is located at the center of the network arena and evaluate its STP under the NNT and NRT schemes, respectively.

1) NNT: Without loss of generality, we focus on a node i and its nearest neighbor node j in an arbitrary time slot. According to the definition of STP, the node i conducts a successful transmission to node j in the time slot iff the following three events happen simultaneously: (i) node i becomes a transmitter; (ii) node j is silent; (iii) the condition of correct reception specified by the protocol interference model in (1) holds. We use indicator function $\delta_{i,j} = 1$ to denote that the condition in (1) is true for the transmission from i to j ($\delta_{i,j} = 0$, otherwise). Due to the i.i.d. mobility model and the A-Aloha protocol, the above three events are mutually independent in $\mathcal{N}_A$, so the STP P_S under NNT is given by

$$P_S = p(1-p)\Pr\{\delta_{i,j} = 1\} = p(1-p)\mathbb{E}\{\delta_{i,j}\}. \tag{16}$$

Let $\mathbb{E}\left\{\delta_{i,j} | d_{ij} = r\right\}$ denote the expectation of $\delta_{i,j}$ conditioned on $d_{ij} = r$, we have

$$\mathbb{E}\{\delta_{i,j}\} = \int_0^{\frac{\sqrt{2}}{2}} \mathbb{E}\left\{\delta_{i,j} | d_{ij} = r\right\} f_{R_1}(r)\, \mathrm{d}r, \tag{17}$$

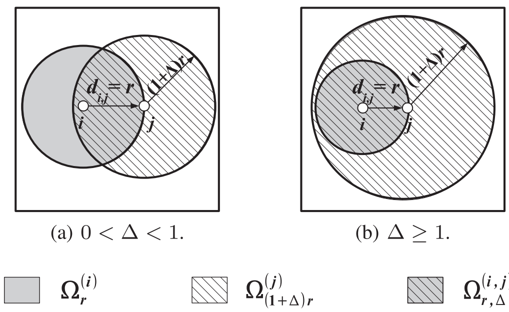

Fig. 2. Illustration of $\Omega_r^{(i)}$, $\Omega_{(1+\Delta)r}^{(j)}$ and $\Omega_{r,\Delta}^{(i,j)}$.

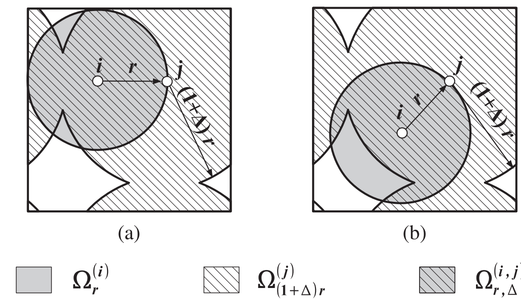

Fig. 3. $\Omega_{r,\Delta}^{(i,j)}$ when $0 < \Delta < 1$ and $\frac{1}{3+\Delta} < r \le \frac{\sqrt{2}}{2}$. In the diagrams Δ and r are the same but the $|\Omega_{r,\Delta}^{(i,j)}|$ are different.

where $\frac{\sqrt{2}}{2}$ is the maximum distance between the transmitter and receiver over a unit square and $f_{R_1}(r)$ denotes the probability density function of the distance between a node and its nearest neighbor in the A-MANET under the i.i.d. mobility model (See, Appendix A. Based on the evaluation of $\mathbb{E}\{\delta_{i,j}|d_{ij}=r\}$, P_{S} can be modeled as follows.

Lemma 3: Considering the A-MANET $\mathcal{N}_A$ with n mobile nodes, transmission probability p and guard interval $\Delta > 0$, it STP P_{S} under the NNT scheme can be evaluated as

$$P_{\mathrm{S}} = \int_0^{\frac{\sqrt{2}}{2}} \sum_{k=0}^{n-2} \binom{n-2}{k} p^{k+1} \left(P_{i,j}(\Delta, r)\right)^k (1-p)^{n-1-k} \cdot f_{R_1}(r)\,\mathrm{d}r, \tag{18}$$

$$P_{i,j}(\Delta, r) = \frac{1 - |\Omega_r^{(i)}| - |\Omega_{(1+\Delta)r}^{(j)}| + |\Omega_{r,\Delta}^{(i,j)}|}{1 - |\Omega_r^{(i)}|}, \tag{19}$$

where $\Omega_r^{(a)}$ is the intersection between the network region and the disc centered at node a with radius r, $\Omega_{r,\Delta}^{(i,j)}$ is the intersection between $\Omega_r^{(i)}$ and $\Omega_{(1+\Delta)r}^{(j)}$ (Fig. 2) and $|\cdot|$ is the region area.

Proof: At first, we evaluate $\mathbb{E}\{\delta_{i,j}|d_{ij}=r\}$. As illustrated in Fig. 2, $\mathbb{E}\{\delta_{i,j}|d_{ij}=r\}$ accounts for the probability that all transmitting nodes other than i are outside of $\Omega_{(1+\Delta)r}^{(j)}$ given that all nodes other than i and j are outside of $\Omega_r^{(i)}$. Denoting k the number of transmitters other than i and j, we have from the i.i.d. mobility model and A-Aloha protocol that k follows the Binomial distribution with parameters p and $n-2$. Let $P_{i,j}$ denote the probability that a node is outside of $\Omega_{(1+\Delta)r}^{(j)}$ given that it is outside of $\Omega_r^{(i)}$, then we have from the law of total probability

$$\mathbb{E}\{\delta_{i,j}|d_{ij}=r\} = \sum_{k=0}^{n-2} \binom{n-2}{k} (p\cdot P_{i,j}(\Delta, r))^k (1-p)^{n-2-k}. \tag{20}$$

Combining (16), (17) and (20) completes the proof of the lemma. ■

Lemma 3 indicates that we need to determine $|\Omega_r^{(i)}|$, $|\Omega_{(1+\Delta)r}^{(j)}|$ and $|\Omega_{r,\Delta}^{(i,j)}|$ to evaluate $\mathbb{E}\{\delta_{i,j}|d_{ij}=r\}$. Since $|\Omega_r^{(i)}|$ and $|\Omega_{(1+\Delta)r}^{(j)}|$ can be easily determined based on (36) in Appendix A, the remaining issue is to determine $|\Omega_{r,\Delta}^{(i,j)}|$. As illustrated in Fig. 2, when $0 < \Delta < 1$, $\Omega_r^{(i)}$ and $\Omega_{(1+\Delta)r}^{(j)}$ are partially overlapped, but when $\Delta \ge 1$, $\Omega_r^{(i)}$ is completely contained in $\Omega_{(1+\Delta)r}^{(j)}$. The different overlapping behaviors of these two cases make the calculation of $|\Omega_{r,\Delta}^{(i,j)}|$ different, so we need to consider them separately. In the following, we focus on the case of $0 < \Delta < 1$. The evaluation for $\Delta \ge 1$ can be conducted similarly (Appendix B). Notice that in addition to Δ, $|\Omega_{r,\Delta}^{(i,j)}|$ also depends on r. When $(3+\Delta)r \le 1$ (or equivalently $0 < r \le \frac{1}{3+\Delta}$), $\Omega_{r,\Delta}^{(i,j)}$ just corresponds to the intersection between two discs illustrated in Fig. 2a, so $|\Omega_{r,\Delta}^{(i,j)}|$ can be easily evaluated under this scenario. However, under the scenario when $(3+\Delta)r > 1$ (or equivalently $\frac{1}{3+\Delta} < r \le \frac{\sqrt{2}}{2}$), it is quite cumbersome to compute $|\Omega_{r,\Delta}^{(i,j)}|$, due to that the torus causes the two discs to overlap with one another in irregular and unsavory manners illustrated in Fig. 3.

Based on the above discussion, for the case of $0 < \Delta < 1$, $\mathbb{E}\left\{\delta_{i,j}\right\}$ in (17) is evaluated as

$$\mathbb{E}\{\delta_{i,j}\} = \underbrace{\int_0^{\frac{1}{3+\Delta}} \mathbb{E}\left\{\delta_{i,j}|d_{ij}=r\right\} f_{R_1}(r)\,\mathrm{d}r}_{(a)} + \underbrace{\int_{\frac{1}{3+\Delta}}^{\frac{\sqrt{2}}{2}} \mathbb{E}\left\{\delta_{i,j}|d_{ij}=r\right\} f_{R_1}(r)\,\mathrm{d}r}_{(b)}, \tag{21}$$

in which (a) can be analytically derived while the analysis of (b) is highly cumbersome due to the difficulty in computing $|\Omega_{r,\Delta}^{(i,j)}|$. Fortunately, as proved in Appendix B, the (b) in (21) accounts for an increasingly negligible part as n increases. Intuitively, as n increases (i.e., adding more nodes to the network), the nearest neighbor distribution tends to tighten up towards zero, causing smaller distances between a transmitter and receiver. It follows from (1) that smaller distances between a transmitter and receiver lead to smaller guard zones, and since the network arena size is fixed, smaller guard zones decrease the chance of having unsavory overlaps.

Lemma 4: Considering the A-MANET $\mathcal{N}_A$ with n mobile nodes, transmission probability p and guard interval $\Delta > 0$, its STP P_{S} under the NNT scheme is given by

$$P_{\mathrm{S}} = \widehat{P}_{\mathrm{S}} + \Theta(\alpha^n),\ 0 < \alpha < 1, \tag{22}$$

$$\widehat{P}_{\mathrm{S}} = \begin{cases} \frac{\pi p(1-p)}{\pi + p\cdot\Psi(\Delta)}, & \text{if } 0 < \Delta < 1 \\ \frac{p(1-p)}{1+2\Delta p+\Delta^2 p}, & \text{if } \Delta \ge 1 \end{cases}, \tag{23}$$

$$\Psi(\Delta) = \pi(1+\Delta)^2 - (1+\Delta)^2 \arccos\left(\frac{1+\Delta}{2}\right) - \arccos\left(1 - \frac{(1+\Delta)^2}{2}\right) + (1+\Delta)\sqrt{1 - \frac{(1+\Delta)^2}{4}}. \quad (24)$$

Proof: See Appendix B. ■

2) NRT: Following an argument similar to that of NNT, we have the following result.

Lemma 5: Considering the A-MANET $\mathcal{N}_A$ with n mobile nodes, transmission probability p and guard interval $\Delta > 0$, its STP P_S under the NRT scheme is given by

$$P_S = \widehat{P}_S + \Theta(\alpha^n), \quad (25)$$

where $0 < \alpha < 1$ and $\widehat{P}_S = \frac{p(1-p)}{1+2\Delta p+\Delta^2 p}$.

Proof: See Appendix C. ■

Remark 1: Lemmas 4 and 5 indicate that for both NNT and NRT schemes, the STP P_S of $\mathcal{N}_A$ consists of two parts. The first part is $\widehat{P}_S$, which is independent of n. The second part is of order $\Theta(\alpha^n)$, which vanishes to 0 exponentially with n. Thus, we have $\lim_{n\to\infty} P_S = \widehat{P}_S$ for the A-MANET $\mathcal{N}_A$ under the NNT or NRT scheme.

Remark 2: Notice that when $\Delta \geq 1$ the NNT and NRT schemes result in the same expression of $\widehat{P}_S$. This is because under the NNT scheme, a transmitter can only conduct nearest-neighbor transmissions, while under the NRT scheme, a transmitter can conduct either nearest-neighbor transmissions (where the nearest receiver is just its nearest neighbor) or non-nearest-neighbor transmissions (where the nearest receiver is not its nearest neighbor). Under the case of $\Delta \geq 1$, however, the non-nearest-neighbor transmissions under the NRT scheme can never satisfy the condition of correct reception specified by the protocol interference model. This is because when $\Delta \geq 1$, the disc centered at the transmitter with radius r is completely covered by the disc centered at the receiver with radius $(1+\Delta)r$, as illustrated in Fig. 2b. Thus, if the nearest receiver under NRT is not the nearest neighbor of the transmitter under this case, it implies that there must be some other transmitting node(s) in the disc centered at the transmitter (hence in the disc centered at the receiver of this transmission), making this transmission fail.

B. Throughput Capacity

Based on Theorems 1, 2 and Remark 1, we have the following theorem.

Theorem 3: Consider the A-MANET $\mathcal{N}_A$ or $\mathcal{N}_C$ with n mobile nodes, transmission probability p and guard interval $\Delta > 0$. If we use μ_{NNT} and μ_{NRT} to denote its throughput capacity under the NNT and NRT schemes and μ^∞_{NNT} and μ^∞_{NRT} to denote the throughput capacity of the corresponding infinite network, respectively, then we have

$$\mu^\infty_{\text{NNT}} = \lim_{n\to\infty} \mu_{\text{NNT}} = \begin{cases} \frac{\pi p(1-p)}{2\pi+2p\cdot\Psi(\Delta)}, & \text{if } 0 < \Delta < 1 \\ \frac{p(1-p)}{2+4\Delta p+2\Delta^2 p}, & \text{if } \Delta \geq 1 \end{cases} \quad (26)$$

$$\mu^\infty_{\text{NRT}} = \lim_{n\to\infty} \mu_{\text{NRT}} = \frac{p(1-p)}{2+4\Delta p+2\Delta^2 p}. \quad (27)$$

Theorem 3 indicates that under either the NNT or NRT scheme, the throughput capacity of the A-MANETs will converge to a constant value as n grows to infinity. Moreover, the convergence is exponential according to Lemmas 4 and 5.

VI. Throughput Capacity of Finite Network

This section derives closed-form approximations to the STP P_S of $\mathcal{N}_A$ and the throughput capacity of a finite $\mathcal{N}_A$ or $\mathcal{N}_C$, and determines the corresponding approximation error bounds. Optimization is also conducted to find the optimal values of p for capacity maximization.

A. STP Approximation and Error Bound

According to Lemmas 4 and 5, the STP P_S consists of a constant part whose analytical expression can be derived and an exponentially vanishing part whose analytical expression is difficult to derive. This observation provides us a way to approximate the STP P_S in the A-MANET $\mathcal{N}_A$ as follows. The analysis on error bounds is provided in Appendices B and C, and the actual values of the bounds are reported in Appendix D.

Corollary 1: Considering the $\mathcal{N}_A$ with n mobile nodes, transmission probability p and guard interval $\Delta > 0$, an approximation $\widehat{P}_S$ to its STP P_S under the NNT scheme is given by

$$\widehat{P}_S = \begin{cases} \frac{\pi p(1-p)}{\pi+p\cdot\Psi(\Delta)}, & \text{if } 0 < \Delta < 1 \\ \frac{p(1-p)}{1+2\Delta p+\Delta^2 p}, & \text{if } \Delta \geq 1 \end{cases}, \quad (28)$$

where the corresponding approximation error $\epsilon_P := P_S - \widehat{P}_S$ vanishes to zero exponentially with n and is bounded as $\epsilon^- \leq \epsilon_P \leq \epsilon^+$. See (49) and (50) for the expressions of ϵ^- and ϵ^+.

Corollary 2: Considering the $\mathcal{N}_A$ with n mobile nodes, transmission probability p and guard interval $\Delta > 0$, an approximation $\widehat{P}_S$ to its STP P_S under the NRT scheme is given by

$$\widehat{P}_S = \frac{p(1-p)}{1+2\Delta p+\Delta^2 p}, \quad (29)$$

where the corresponding approximation error $\epsilon_P := P_S - \widehat{P}_S$ vanishes to zero exponentially with n and is bounded as $\epsilon^- \leq \epsilon_P \leq \epsilon^+$. See (51) and (52) for the expressions of ϵ^- and ϵ^+.

B. Throughput Capacity Approximation and Optimization

The combination of Theorems 1 and 2 and Corollaries 1 and 2 leads to the following results.

Theorem 4: For the $\mathcal{N}_A$ or $\mathcal{N}_C$ with n mobile nodes, transmission probability p and guard interval $\Delta > 0$, an approximation $\widehat{\mu}_{\text{NNT}}$ to its throughput capacity μ_{NNT} under NNT is given by

$$\widehat{\mu}_{\text{NNT}} = \frac{n}{2(n-1)}\widehat{P}_S = \begin{cases} \frac{n\pi p(1-p)}{2(n-1)(\pi+p\cdot\Psi(\Delta))}, & \text{if } 0 < \Delta < 1 \\ \frac{np(1-p)}{2(n-1)(1+2\Delta p+\Delta^2 p)}, & \text{if } \Delta \geq 1 \end{cases}, \quad (30)$$

where the approximation error $\epsilon_\mu = \frac{n}{2(n-1)}\epsilon_P$, and ϵ_P is the approximation error in Corollary 1.

Corollary 3: Let $\widehat{p}^*_{\mathrm{NNT}}$ denote the optimal setting of p to achieve $\widehat{\mu}^*_{\mathrm{NNT}} = \max_{p\in(0,1)} \widehat{\mu}_{\mathrm{NNT}}$. We have from (30) that $\widehat{p}^*_{\mathrm{NNT}}$ and $\widehat{\mu}^*_{\mathrm{NNT}}$ are determined as

$$\widehat{p}^*_{\mathrm{NNT}} = \begin{cases} \frac{\sqrt{\pi^2+\pi\cdot\Psi(\Delta)}-\pi}{\Psi(\Delta)}, & \text{if } 0 < \Delta < 1 \\ \frac{1}{2+\Delta}, & \text{if } \Delta \geq 1 \end{cases}, \tag{31}$$

$$\widehat{\mu}^*_{\mathrm{NNT}} = \begin{cases} \frac{n\pi}{2(n-1)\left[\Psi(\Delta)+2\left(\pi+\sqrt{\pi^2+\pi\cdot\Psi(\Delta)}\right)\right]}, & \text{if } 0 < \Delta < 1 \\ \frac{n}{2(n-1)(2+\Delta)^2}, & \text{if } \Delta \geq 1. \end{cases} \tag{32}$$

Theorem 5: For the $\mathcal{N}_A$ or $\mathcal{N}_C$ with n mobile nodes, transmission probability p and guard interval $\Delta > 0$, an approximation $\widehat{\mu}_{\mathrm{NRT}}$ to its throughput capacity μ_{NRT} under NRT is given by

$$\widehat{\mu}_{\mathrm{NRT}} = \frac{np(1-p)}{2(n-1)(1+2\Delta p+\Delta^2 p)}, \tag{33}$$

where the approximation error $\epsilon_\mu = \frac{n}{2(n-1)}\epsilon_P$, and ϵ_P is the approximation error in Corollary 2.

Corollary 4: Let $\widehat{p}^*_{\mathrm{NRT}}$ denote the optimal setting of p to achieve $\widehat{\mu}^*_{\mathrm{NRT}} = \max_{p\in(0,1)} \widehat{\mu}_{\mathrm{NRT}}$, we have from (33) that $\widehat{p}^*_{\mathrm{NRT}}$ and $\widehat{\mu}^*_{\mathrm{NRT}}$ are determined as

$$\widehat{p}^*_{\mathrm{NRT}} = \frac{1}{2+\Delta} \text{ and } \widehat{\mu}^*_{\mathrm{NRT}} = \frac{n}{2(n-1)(2+\Delta)^2}. \tag{34}$$

VII. Numerical Results and Discussions

A. Simulation Setting

To validate the theoretical results, a self-developed simulator was used to simulate the packet delivery process under Algorithm 1 [35]. A simulation scenario with $p = 0.4$, $\Delta = 0.2$ and unit network arena of 1×1 is considered. To obtain the simulated throughput capacity, we first measure the STP P_S as the time average number of successful transmissions of a specific node over 10^6 time slots in the $\mathcal{N}_C$, and then substitute the measured P_S into (2). To measure the throughput and delay, we focus on a traffic flow and measure its throughput and average packet delay over a period of 10^7 time slots for each system load $\rho = \lambda/\hat{\mu}_{\mathrm{NNT}}$ or $\rho = \lambda/\hat{\mu}_{\mathrm{NRT}}$. In addition to the i.i.d. mobility model, we also implemented the following two models.

Random Direction Model [36]: Initially, network nodes are uniformly distributed over the network arena, and each node independently selects a direction θ uniformly from $(0, 2\pi]$, a speed S uniformly from $[v_{min}, v_{max}]$ and a travel time τ following the Poisson distribution with mean $\bar{\tau} > 0$. The node then travels along the direction θ at speed S for a duration τ. When a travel time has expired, a new setting of θ, S and τ is selected at random, independently of previous ones. When a node reaches a boundary, it is bounced back with angle θ or $\pi - \theta$.

Random Walk Model [37]: Initially, network nodes are uniformly distributed over the network arena. At the beginning of each time slot, each node independently and uniformly selects a speed S from $[v_{min}, v_{max}]$ and a direction θ from $(0, 2\pi]$, and it conducts a movement of $(S \cdot \cos\theta, S \cdot \sin\theta)$. When a node reaches a boundary, it is bounced back with angle θ or $\pi - \theta$.

It is proved in [36] that for a general random direction model, the steady-state distribution of nodes locations is uniform under arbitrary distributions of direction, travel speed and travel time. Notice that in the random walk model, a node always conducts a movement of unit distance before changing directions, so it can be regarded as a special case of the general random direction model. Therefore, both of the above mobility models will lead to a uniform distribution of nodes locations in steady state.

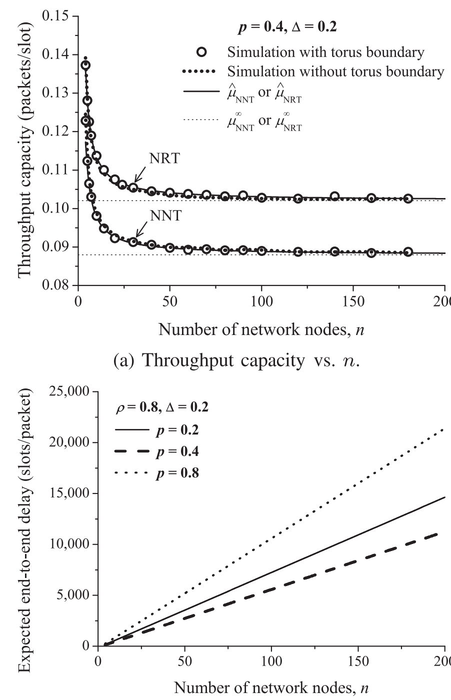

(a) Throughput capacity vs. n.

(b) $\mathbb{E}\{D\}$ vs. n under the NNT scheme.

Fig. 4. Throughput Capacity and Delay vs. Number of Nodes n.

B. Throughput Capacity and Delay vs. Number of Nodes n

To verify our throughput capacity results, we summarize in Fig. 4a the simulation and theoretical results of throughput capacity as functions of n. Fig. 4a shows that the simulation results agree well with the approximations, indicating that (30) and (33) can accurately approximate the throughput capacity of finite A-MANETs. Fig. 4a also shows that the throughput capacity results with the torus assumption are virtually indistinguishable from those without this assumption, indicating that the torus assumption does not incur a significant loss of accuracy here. We can see from Fig. 4a that as n increases the throughput capacity under the NNT or NRT scheme will converge to that of infinite networks. This observation agrees with Theorem 3, and it indicates that the considered A-MANET can provide a constant throughput capacity even as n grows to infinity. To understand the corresponding average delay to achieve the throughput capacity, we examine in Fig. 4b how the delay under Algorithm 1 and the NNT scheme varies with n for the settings of $\rho = 0.8$, $\Delta = 0.2$ and $p = \{0.2, 0.4, 0.8\}$. Here, the delay is computed from (11). Figs. 4a and 4b indicate that a constant throughput capacity can be achieved in the A-MANET at the cost of a linearly increasing average delay.

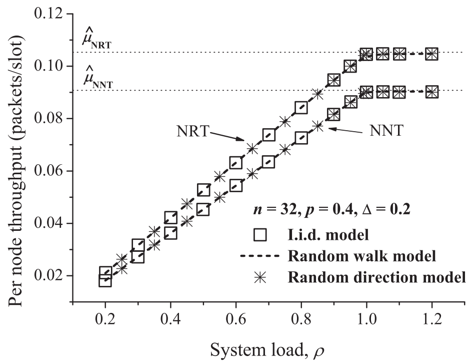

(a) Throughput vs. ρ.

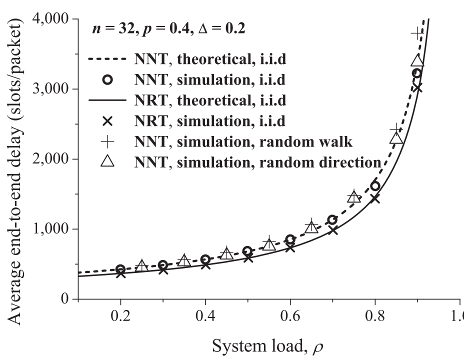

(b) $\mathbb{E}\{D\}$ vs. ρ.

Fig. 5. Throughput and Delay vs. System Load ρ with $v_{min} = 0.1$ per slot, $v_{max} = 0.2$ per slot and $\bar{\tau} = 10$ slots.

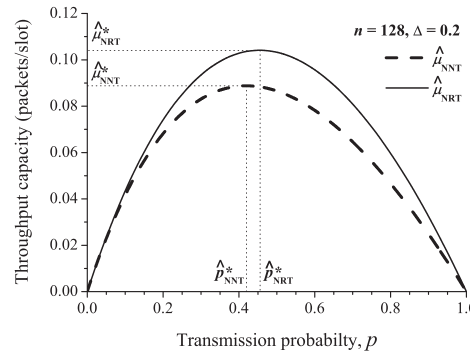

(a) μ_{NNT} and μ_{NRT} vs. p.

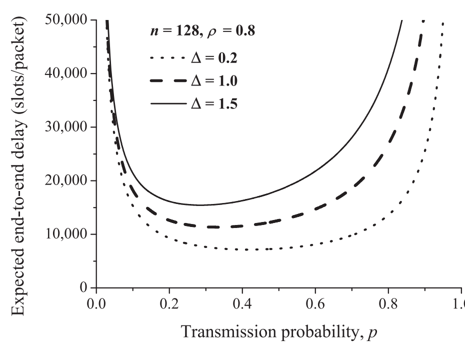

(b) $\mathbb{E}\{D\}$ vs. p under the NNT scheme.

Fig. 6. Throughput Capacity and Delay vs. Transmission Probability p.

C. Throughput and Delay vs. System Load ρ

To demonstrate the throughput and delay performance as input rate approaches throughput capacity, we summarized in Fig. 5 the plots of throughput and delay versus system load ρ for a network with $n = 32$, $p = 0.4$ and $\Delta = 0.2$.[3] Fig. 5a show that for the A-MANET under i.i.d. mobility model, the throughput linearly increases as ρ increases from 0 to 1 and then approaches $\hat{\mu}_{NNT}$ or $\hat{\mu}_{NRT}$ as ρ further increases beyond 1. This is expected since the queuing system of the network is underloaded when $\rho < 1$, and it saturates as ρ approaches 1 and beyond. Fig. 5b indicates that (11) is accurate in reporting the average delay under the i.i.d. mobility model.

Besides, we also provide in Fig. 5 the simulation results of throughput and delay for the random walk and random direction models with the setting of $v_{min} = 0.1$ per slot, $v_{max} = 0.2$ per slot and $\bar{\tau} = 10$ slots. Fig. 5a shows that for networks under the random walk and random direction models, their throughputs also approach the theoretical throughput capacity derived based on the i.i.d. model as ρ tends to 1. This observation suggests that while the throughput capacity result of this paper is developed based on the i.i.d. model, it also severs as a good estimation to the throughput capacity of the A-MANETs under the random walk and random direction models. This might be for the reason that these models lead to the same uniform distribution of nodes locations in steady-state as the i.i.d. model (see Corollary 5 of [30]. Fig. 5b shows that the mean delays under these mobility models are lower bounded by that under the i.i.d. model.

[3]The theoretical results are obtained from $\hat{\mu}_{NNT}$, $\hat{\mu}_{NRT}$ and (11).

D. Throughput Capacity and Delay vs. Transmission Probability p

Based on our theoretical results, we explore the impact of p on the throughput capacity. It is summarized in Fig. 6a how $\hat{\mu}_{NNT}$ and $\hat{\mu}_{NRT}$ vary with p in a network with $n = 128$ and $\Delta = 0.2$. Fig. 6a shows that as p increases both $\hat{\mu}_{NNT}$ and $\hat{\mu}_{NRT}$ first increase and then decrease, and just as discussed in Corollaries 3 and 4 that there exists an optimal setting of p to achieve the maximum capacity $\widehat{\mu}^*_{NNT}$ or $\widehat{\mu}^*_{NRT}$. This is mainly due to the reason that the effects of p on throughput capacity are two-fold. On one hand, a higher transmission probability will result in a larger number of simultaneous transmissions, but on the other hand, it will lead to a lower probability that a transmission is successfully received. Fig. 6a also indicates that for a given setting of p the throughput capacity under the NRT scheme is always higher than that under the NNT scheme. This is because under the NRT scheme a transmitter will try to find some other node as its receiver if the nearest neighbor is not available, so more transmission opportunities can be obtained. To further explore the effect of p on delay performance, we summarize in Fig. 6b how the delay varies with p under the settings of $n = 128$, $\rho = 0.8$ and $\Delta = \{0.2, 1.0, 1.5\}$. Fig. 6b shows that for a given setting of n, ρ and Δ, as p increases the delay first decreases and then increases; while for a given setting of n, ρ and p, the delay monotonously increases as Δ increases. The main reason behind these phenomena is that as shown in (11) the delay is inversely proportional to the capacity, so the relationship between delay and (p, Δ) is just reverse to the relationship between capacity and (p, Δ) shown in Fig. 6a.

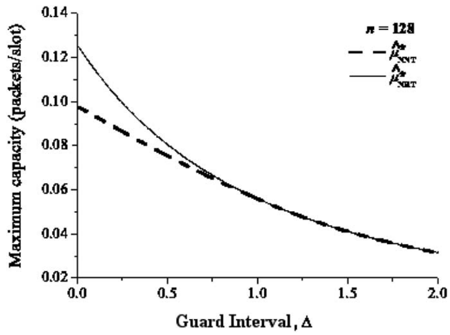

Fig. 7. Maximum Capacity vs. Guard Interval Δ.

E. Maximum Capacity vs. Guard Interval Δ

Fig. 6a shows that for a given n and Δ, there exist maximum capacities $\widehat{\mu}^*_{\mathrm{NNT}}$ and $\widehat{\mu}^*_{\mathrm{NRT}}$ under the NNT and NRT schemes, respectively. To understand the impact of Δ on the maximum capacity of A-MANETs, it is summarized in Fig. 7 how $\widehat{\mu}^*_{\mathrm{NNT}}$ and $\widehat{\mu}^*_{\mathrm{NRT}}$ vary with Δ in a network of $n = 128$. Fig. 7 shows that as Δ increases both $\widehat{\mu}^*_{\mathrm{NNT}}$ and $\widehat{\mu}^*_{\mathrm{NRT}}$ monotonously decrease. This is mainly due to the reason that under the protocol interference model (1), a larger value of Δ will lead to a lower probability that a transmission is successfully received and thus a smaller capacity. Another observation of Fig. 7 is that as Δ increases, the gap between $\widehat{\mu}^*_{\mathrm{NNT}}$ and $\widehat{\mu}^*_{\mathrm{NRT}}$ quickly vanishes and becomes zero when Δ is larger than 1. This is because under the NRT scheme, increasing Δ will lead to a decrease in the successful probability of the non-nearest-neighbor transmissions and thus a reduction of capacity improvement $\widehat{\mu}^*_{\mathrm{NRT}} - \widehat{\mu}^*_{\mathrm{NNT}}$. Specifically, as discussed in Remark 1, when $\Delta \geq 1$, the successful probability of non-nearest-neighbor transmissions becomes 0 and thus no capacity improvement can be obtained by adopting NRT.

VIII. Conclusion

This paper represents the first attempt to derive the closed-form expressions for the throughput capacity of A-MANETs. The theoretical framework and results developed in this paper are expected to be helpful not only for understanding the fundamental throughput performance of A-MANETs but also for initiating the exact capacity evaluation for other MANET scenarios. Some interesting findings of this work are: 1) while the theoretical capacity expressions were developed under the i.i.d. mobility model, they also serve as a good estimation to the throughput capacity of the A-MANETs with the more practical random walk and random direction mobility models; 2) the throughput capacity of the A-MANETs will converge to a constant as the number of network nodes grows to infinity; 3) for capacity maximization in the A-MANETs, the optimal setting of transmission probability in the Aloha protocol mainly depends on guard zone parameter and is not sensitive to the number of network nodes. In this paper, only unicast traffic scenario is investigated, so one possible future direction is to conduct exact throughput capacity analysis for A-MANETs with multicast traffic where a source may communicate with multiple destinations. Another future direction is to extend the study of this paper to conduct throughout capacity study for A-MANETs under the more realistic SINR model.

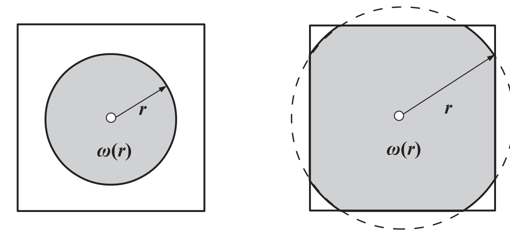

(a) $0 \leq r \leq \frac{1}{2}$. (b) $\frac{1}{2} < r \leq \frac{\sqrt{2}}{2}$.

Fig. 8. Illustration of $\omega(r)$ represented by the gray area in the figure.

Appendix A
Node Distance Analysis

Following the method of [38], we derive the probability density function of the distance between the tagged node and its k-th nearest neighbor.

Lemma 6: For an A-MANET with n mobile nodes, we use R_k $(0 < k \leq n-1)$ to denote the distance between the tagged node and its k-th nearest neighbor at a time slot, then its probability density function $f_{R_k}(r)$ is determined as

$$f_{R_k}(r) = \frac{\omega'(r)\,(\omega(r))^{k-1}\,(1-\omega(r))^{n-k-1}}{B(k, n-k)}, \tag{35}$$

$$\omega(r) = \begin{cases} \pi r^2 & 0 \leq r \leq \frac{1}{2} \\ \pi r^2 - 4r^2 \mathrm{arcsec}(2r) + \sqrt{4r^2 - 1} & \frac{1}{2} < r \leq \frac{\sqrt{2}}{2} \end{cases}, \tag{36}$$

$\omega'(r)$ is the derivative of $\omega(r)$ and $B(x, y) = \frac{\Gamma(x)\Gamma(y)}{\Gamma(x+y)}$ is the beta function.

Proof: Let $\omega(r)$ denote the intersection between the disc centered at the tagged node with radius r and the network arena.[4] Since the network arena is a unit square, $\omega(r)$ can be determined by considering the cases $0 \leq r \leq \frac{1}{2}$ and $\frac{1}{2} < r \leq \frac{\sqrt{2}}{2}$ illustrated in Figs. 8 and 8b, respectively. Let N_r denote the number of nodes (excluding the tagged one) that fall within $\omega(r)$ in the current time slot, we can see that N_r follows the Binomial distribution with parameters $n-1$ and $\omega(r)$. Notice that a node falls within $\omega(r)$ iff its distance to the concerned node is no larger than r, so the cumulative density function $F_{R_k}(r)$ of R_k is given by

$$\begin{aligned} F_{R_k}(r) &= \Pr\{R_k \leq r\} \\ &= \Pr\{N_r \geq k\} = \sum_{t=k}^{n-1} \binom{n-1}{t} (\omega(r))^t (1-\omega(r))^{n-1-t} \\ &= I_{\omega(r)}(k, n-k), \end{aligned} \tag{37}$$

where $I_x(a, b)$ is the regularized incomplete beta function. Taking derivative with respect to r in both sides of (37), the formula (35) then follows. ∎

Appendix B
Proof of Lemma 4

1) Case of $0 < \Delta < 1$: Based on the discussion in Section V-A, $\mathbb{E}\{\delta_{i,j}\}$ can be evaluated as (21), where (a) can be derived as follows. At first we have from geometric calculations

[4] For simplicity, we use $\omega(r)$ to denote both the intersection and its area.

$$\begin{aligned}|\Omega_r^{(i)}| &= \pi r^2,\\ |\Omega_{(1+\Delta)r}^{(j)}| &= \pi(1+\Delta)^2 r^2,\\ |\Omega_{r,\Delta}^{(i,j)}| &= r^2(1+\Delta)^2 \arccos\left(\frac{1+\Delta}{2}\right)\\ &\quad + r^2 \arccos\left(1-\frac{(1+\Delta)^2}{2}\right)\\ &\quad - r^2(1+\Delta)\sqrt{1-\frac{(1+\Delta)^2}{4}}.\end{aligned} \tag{38}$$

Based on (38), (19) and (20), the term $\mathbb{E}\{\delta_{i,j}|d_{ij}=r\}$ in integration (a) can be evaluated as

$$\mathbb{E}\{\delta_{i,j}|d_{ij}=r\} = \left(1 - p\cdot\frac{\pi(1+\Delta)^2r^2 - |\Omega_{r,\Delta}^{(i,j)}|}{1-\pi r^2}\right)^{n-2} \tag{39}$$

Based on (39) and Lemma 6, (a) can be evaluated as

$$\begin{aligned}&\int_0^{\frac{1}{3+\Delta}} \mathbb{E}\left\{\delta_{i,j}|d_{ij}=r\right\} f_{R_1}(r)\,\mathrm{d}r\\ &= 2\pi(n-1)\int_0^{\frac{1}{3+\Delta}} r\left(1-(\pi+p\cdot\Psi(\Delta))r^2\right)^{n-2}\mathrm{d}r\\ &= \frac{\pi}{\pi+p\cdot\Psi(\Delta)} - \underbrace{\frac{\pi}{\pi+p\cdot\Psi(\Delta)}\left(1-\frac{\pi+p\cdot\Psi(\Delta)}{(3+\Delta)^2}\right)^{n-1}}_{(c)}\end{aligned} \tag{40}$$

As discussed in Section V-A, the evaluation of integration (b) is quite cumbersome. However, we notice that the term $\mathbb{E}\left\{\delta_{i,j}|d_{ij}=r\right\}$ is monotonically decreasing. From the second mean value theorem for integration, we know that there exists a $\xi \in (\frac{1}{3+\Delta}, \frac{\sqrt{2}}{2}]$ such that

$$\begin{aligned}0 &\le \int_{\frac{1}{3+\Delta}}^{\frac{\sqrt{2}}{2}} \mathbb{E}\left\{\delta_{i,j}|d_{ij}=r\right\} f_{R_1}(r)\,\mathrm{d}r\\ &= \mathbb{E}\left\{\delta_{i,j}|d_{ij}=\frac{1}{3+\Delta}\right\}\int_{\frac{1}{3+\Delta}}^{\xi} f_{R_1}(r)\,\mathrm{d}r\\ &\le \mathbb{E}\left\{\delta_{i,j}|d_{ij}=\frac{1}{3+\Delta}\right\}\left(1-F_{R_1}\left(\frac{1}{3+\Delta}\right)\right)\\ &= \underbrace{\left(1-p\cdot\frac{\Psi(\Delta)}{(3+\Delta)^2-\pi}\right)^{n-2}\left(1-\frac{\pi}{(3+\Delta)^2}\right)^{n-1}}_{(d)}.\end{aligned} \tag{41}$$

Since (c) and (d) exponentially vanish with n, the lemma follows by denoting $\widehat{P}_{\mathrm{S}} = \frac{\pi p(1-p)}{\pi+p\cdot\Psi(\Delta)}$.

2) Case of $\Delta \ge 1$: Under this case $\mathbb{E}\{\delta_{i,j}\}$ can be evaluated as

$$\begin{aligned}\mathbb{E}\{\delta_{i,j}\} &= \int_0^{\frac{1}{2+2\Delta}} \mathbb{E}\left\{\delta_{i,j}|d_{ij}=r\right\} f_{R_1}(r)\,\mathrm{d}r\\ &\quad + \int_{\frac{1}{2+2\Delta}}^{\frac{\sqrt{2}}{2}} \mathbb{E}\left\{\delta_{i,j}|d_{ij}=r\right\} f_{R_1}(r)\,\mathrm{d}r.\end{aligned}$$

In the first integration, the term $\mathbb{E}\{\delta_{i,j}|d_{ij}=r\}$ is derived as

$$\mathbb{E}\{\delta_{i,j}|d_{ij}=r\} = \left(1-p\cdot\frac{\pi(1+\Delta)^2r^2-\pi r^2}{1-\pi r^2}\right)^{n-2}. \tag{42}$$

Hence,

$$\begin{aligned}&\int_0^{\frac{1}{2+2\Delta}} \mathbb{E}\left\{\delta_{i,j}|d_{ij}=r\right\} f_{R_1}(r)\,\mathrm{d}r\\ &= 2\pi(n-1)\int_0^{\frac{1}{2+2\Delta}} r\left(1-(1+2\Delta p+\Delta^2 p)\pi r^2\right)^{n-2}\mathrm{d}r\\ &= \frac{1}{1+2\Delta p+\Delta^2 p}\left(1-\left(1-\frac{(1+2\Delta p+\Delta^2 p)\pi}{(2+2\Delta)^2}\right)^{n-1}\right).\end{aligned} \tag{43}$$

In the second integration, the evaluation of $\mathbb{E}\{\delta_{i,j}|d_{ij}=r\}$ is also quite cumbersome. Following an argument similar to that of (41), we have

$$\begin{aligned}0 &\le \int_{\frac{1}{2+2\Delta}}^{\frac{\sqrt{2}}{2}} \mathbb{E}\left\{\delta_{i,j}|d_{ij}=r\right\} f_{R_1}(r)\,\mathrm{d}r\\ &\le \mathbb{E}\left\{\delta_{i,j}|d_{ij}=\frac{1}{2+2\Delta}\right\}\left(1-F_{R_1}\left(\frac{1}{2+2\Delta}\right)\right)\\ &= \left(1-p\cdot\frac{\pi(1+\Delta)^2-\pi}{(2+2\Delta)^2-\pi}\right)^{n-2}\left(1-\frac{\pi}{(2+2\Delta)^2}\right)^{n-1}.\end{aligned} \tag{44}$$

Denoting $\widehat{P}_{\mathrm{S}} = \frac{p(1-p)}{1+2\Delta p+\Delta^2 p}$, the lemma follows after some basic calculations.

Appendix C
Proof of Lemma 5

Remark 1 indicates that when $\Delta \ge 1$, the NNT and NRT result in the same STP, so it is adequate to prove the case of $0 < \Delta < 1$. Without loss of generality, we focus on a node i in a time slot. We use R_k to denote the distance from node i to its k-th nearest neighbor, B_i to denote the nearest silent node of node i, and $B_i = k$ to indicate that B_i is its k-th nearest neighbor. The event that i can successfully conduct a transmission in the time slot iff the following two events happen simultaneously. First, i becomes a transmitter. Second, the condition of correct reception specified by the protocol interference model of (1) holds for the transmitter i and its nearest silent node B_i. We use indicator function $\delta_{i,B_i} = 1$ to denote that the condition in (1) is true for the transmission from i to B_i ($\delta_{i,B_i} = 0$, otherwise). Since above two events are mutually independent, we can see that STP P_{S} under the NRT scheme is determined as $P_{\mathrm{S}} = p\Pr\{\delta_{i,B_i}=1\} = p\mathbb{E}\{\delta_{i,B_i}\}$. Conditioning on $B_i = k$, we have $\mathbb{E}\{\delta_{i,B_i}\} = \sum_{k=1}^{n-1}\mathbb{E}\{\delta_{i,B_i}|B_i=k\}\cdot\Pr\{B_i=k\}$, where $\Pr\{B_i=k\} = p^{k-1}(1-p)$. Further conditioning on $R_k = r$ and combining the result of Lemma 6, the $\mathbb{E}\{\delta_{i,B_i}\}$ can be evaluated as

$$\begin{aligned}&\mathbb{E}\{\delta_{i,B_i}\}\\ &= \sum_{k=1}^{n-1}\int_0^{\frac{1}{3+\Delta}} \mathbb{E}\{\delta_{i,k}|B_i=k, R_k=r\}\Pr\{B_i=k\}f_{R_k}(r)\,\mathrm{d}r\\ &\quad + \sum_{k=1}^{n-1}\int_{\frac{1}{3+\Delta}}^{\frac{\sqrt{2}}{2}} \mathbb{E}\{\delta_{i,k}|B_i=k, R_k=r\}\Pr\{B_i=k\}f_{R_k}(r)\,\mathrm{d}r.\end{aligned} \tag{45}$$

The term $\mathbb{E}\{\delta_{i,k}|B_i = k, R_k = r\}$ in the first part of (45) can be determined as

$$\begin{aligned}
&\mathbb{E}\{\delta_{i,k}|B_i = k, R_k = r\}\\
&= \left(1 - \frac{|\Omega_{r,\Delta}^{(i,j)}|}{\pi r^2}\right)^{k-1} \sum_{t=0}^{n-k-1} \binom{n-k-1}{t} p^t (1-p)^{n-k-1-t}\\
&\quad \cdot \left(1 - \frac{\pi(1+\Delta)^2 r^2 - |\Omega_{r,\Delta}^{(i,j)}|}{1-\pi r^2}\right)^t\\
&= \left(1 - \frac{|\Omega_{r,\Delta}^{(i,j)}|}{\pi r^2}\right)^{k-1} \left(1 - p \cdot \frac{\pi(1+\Delta)^2 r^2 - |\Omega_{r,\Delta}^{(i,j)}|}{1-\pi r^2}\right)^{n-1-k},
\end{aligned} \tag{46}$$

where $|\Omega_{r,\Delta}^{(i,j)}|$ is given in (38). Hence, the first part of (45) can be determined as

$$\begin{aligned}
&\sum_{k=1}^{n-1} \int_0^{\frac{1}{3+\Delta}} \mathbb{E}\{\delta_{i,k}|B_i = k, R_k = r\} \Pr\{B_i = k\} f_{R_k}(r)\, \mathrm{d}r\\
&= (1-p) \int_0^{\frac{1}{3+\Delta}} 2\pi r \sum_{k=1}^{n-1} \frac{\Gamma(n)}{\Gamma(k)\Gamma(n-k)} \left(p\left(\pi r^2 - |\Omega_{r,\Delta}^{(i,j)}|\right)\right)^{k-1}\\
&\quad \cdot \left(1 - \pi r^2 - p\left(\pi(1+\Delta)^2 r^2 - |\Omega_{r,\Delta}^{(i,j)}|\right)\right)^{n-k-1} \mathrm{d}r\\
&= (1-p) \int_0^{\frac{1}{3+\Delta}} 2\pi r (n-1)(1-(1+2\Delta p+\Delta^2 p)\pi r^2)^{n-2}\, \mathrm{d}r\\
&= \frac{1-p}{1+2\Delta p+\Delta^2 p}\left(1 - \left(1 - \frac{(1+2\Delta p+\Delta^2 p)\pi}{(3+\Delta)^2}\right)^{n-1}\right).
\end{aligned} \tag{47}$$

Similar to (41), the second part of (45) is bounded as

$$\begin{aligned}
&\sum_{k=1}^{n-1} \int_{\frac{1}{3+\Delta}}^{\frac{\sqrt{2}}{2}} \mathbb{E}\{\delta_{i,k}|B_i = k, R_k = r\} \Pr\{B_i = k\} f_{R_k}(r)\, \mathrm{d}r\\
&\le \sum_{k=1}^{n-1} \mathbb{E}\left\{\delta_{i,k}|B_i = k, R_k = \frac{1}{3+\Delta}\right\} \Pr\{B_i = k\}\\
&\quad \cdot \left(1 - F_{R_k}\left(\frac{1}{3+\Delta}\right)\right)\\
&\le \sum_{k=1}^{n-1} \mathbb{E}\left\{\delta_{i,k}|B_i = k, R_k = \frac{1}{3+\Delta}\right\} \Pr\{B_i = k\}\\
&= (1-p) \frac{\left(1 - p\cdot\frac{\Psi(\Delta)}{(3+\Delta)^2-\pi}\right)^{n-1} - \left(p - p\cdot\frac{\Psi(\Delta)-(1+\Delta)^2}{\pi}\right)^{n-1}}{1 - p\left(1 + \frac{\Psi(\Delta)}{(3+\Delta)^2-\pi} - \frac{\Psi(\Delta)-(1+\Delta)^2}{\pi}\right)}.
\end{aligned} \tag{48}$$

Denoting $\widehat{P}_{\mathrm{S}} = \frac{p(1-p)}{1+2\Delta p+\Delta^2 p}$, the lemma follows after some basic calculations.

Appendix D
Approximation Error Bounds

NNT: The approximation error bounds of Corollary 1 are given by

$$\epsilon^- = \begin{cases} -\frac{\pi p(1-p)}{\pi + p\cdot\Psi(\Delta)}\left(1 - \frac{\pi + p\cdot\Psi(\Delta)}{(3+\Delta)^2}\right)^{n-1}, & \text{if } 0 < \Delta < 1\\ -\frac{p(1-p)}{1+2\Delta p+\Delta^2 p}\left(1 - \frac{(1+2\Delta p+\Delta^2 p)\pi}{(2+2\Delta)^2}\right)^{n-1}, & \text{if } \Delta \ge 1 \end{cases} \tag{49}$$

$$\epsilon^+ = \begin{cases} p(1-p)\left[\left(1 - p\cdot\frac{\Psi(\Delta)}{(3+\Delta)^2-\pi}\right)^{n-2}\left(1 - \frac{\pi}{(3+\Delta)^2}\right)^{n-1} \right.\\ \left. -\frac{\pi}{\pi+p\cdot\Psi(\Delta)}\left(1 - \frac{\pi+p\cdot\Psi(\Delta)}{(3+\Delta)^2}\right)^{n-1}\right], & \text{if } 0 < \Delta < 1\\ p(1-p)\left[\left(1 - p\cdot\frac{\pi(1+\Delta)^2-\pi}{(2+2\Delta)^2-\pi}\right)^{n-2}\left(1 - \frac{\pi}{(2+2\Delta)^2}\right)^{n-1}\right.\\ \left. -\frac{1}{1+2\Delta p+\Delta^2 p}\left(1 - \frac{(1+2\Delta p+\Delta^2 p)\pi}{(2+2\Delta)^2}\right)^{n-1}\right], & \text{if } \Delta \ge 1 \end{cases} \tag{50}$$

NRT: The approximation error bounds of Corollary 2 are given by

$$\epsilon^- = -\frac{p(1-p)}{1+2\Delta p+\Delta^2 p}\left(1 - \frac{(1+2\Delta p+\Delta^2 p)\pi}{(3+\Delta)^2}\right)^{n-1}, \tag{51}$$

$$\epsilon^+ = \begin{cases} \frac{p(1-p)}{1-p\left(1+\frac{\Psi(\Delta)}{(3+\Delta)^2-\pi}-\frac{\Psi(\Delta)-(1+\Delta)^2}{\pi}\right)}\left[\left(1 - \frac{p\Psi(\Delta)}{(3+\Delta)^2-\pi}\right)^{n-1}\right.\\ \left. -\left(p - p\cdot\frac{\Psi(\Delta)-(1+\Delta)^2}{\pi}\right)^{n-1}\right] - \frac{p(1-p)}{1+2\Delta p+\Delta^2 p}\\ \cdot\left(1 - \frac{(1+2\Delta p+\Delta^2 p)\pi}{(3+\Delta)^2}\right)^{n-1}, & \text{if } 0 < \Delta < 1\\ p(1-p)\left[\left(1 - p\cdot\frac{\pi(1+\Delta)^2-\pi}{(2+2\Delta)^2-\pi}\right)^{n-2}\left(1 - \frac{\pi}{(2+2\Delta)^2}\right)^{n-1}\right.\\ \left. -\frac{1}{1+2\Delta p+\Delta^2 p}\left(1 - \frac{(1+2\Delta p+\Delta^2 p)\pi}{(2+2\Delta)^2}\right)^{n-1}\right], & \text{if } \Delta \ge 1. \end{cases} \tag{52}$$

References

[1] Y. Chen, Y. Shen, X. Jiang, and J. Li, "Throughput capacity of ALOHA MANETs," in *Proc. IEEE Int. Conf. Commun. China (ICCC)*, 2013, pp. 71–75.

[2] M. Grossglauser and D. N. C. Tse, "Mobility increases the capacity of ad hoc wireless networks," *IEEE/ACM Trans. Netw.*, vol. 10, no. 4, pp. 477–486, Aug. 2002.

[3] J. Andrews, et al., "Rethinking information theory for mobile ad hoc networks," *IEEE Commun. Mag.*, vol. 46, no. 12, pp. 94–101, Dec. 2008.

[4] A. E. Gamal, J. Mammen, B. Prabhakar, and D. Shah, "Optimal throughput-delay scaling in wireless networks—Part II: Constant-size packets," *IEEE Trans. Inf. Theory*, vol. 52, no. 11, pp. 5111–5116, Nov. 2006.

[5] J. Mammen and D. Shah, "Throughput and delay in random wireless networks with restricted mobility," *IEEE Trans. Inf. Theory*, vol. 53, no. 3, pp. 1108–1116, Mar. 2007.

[6] C. Hu, X. Wang, and F. Wu, "Motioncast: On the capacity and delay tradeoffs," in *Proc. ACM MobiHoc*, 2009, pp. 289–298.

[7] X. Wang, W. Huang, S. Wang, J. Zhang, and C. Hu, "Delay and capacity tradeoff analysis for MotionCast," *IEEE/ACM Trans. Netw.*, vol. 19, no. 5, pp. 1354–1367, Oct. 2011.

[8] Y. Qin, X. Tian, W. Wu, and X. Wang, "Mobility weakens the distinction between multicast and unicast," *IEEE/ACM Trans. Netw.*, to be published.

[9] N. Lu and X. S. Shen, "Scaling laws for throughput capacity and delay in wireless networks—A survey," *IEEE Commun. Surveys Tuts.*, vol. 16, no. 2, pp. 642–657, May 2014.

[10] M. Neely and E. Modiano, "Capacity and delay tradeoffs for ad-hoc mobile networks," *IEEE Trans. Inf. Theory*, vol. 51, no. 6, pp. 1917–1937, Jun. 2005.

[11] R. Urgaonkar and M. Neely, "Network capacity region and minimum energy function for a delay-tolerant mobile ad hoc network," *IEEE/ACM Trans. Netw.*, vol. 19, no. 4, pp. 1137–1150, Aug. 2011.

[12] Y. Chen, Y. Shen, J. Zhu, and X. Jiang, "Capacity and delay-throughput tradeoff in ICMNs with Poisson contact process," *Wireless Netw.*, vol. 21, no. 8, pp. 2453–2466, 2015.
[13] G. Mergen and L. Tong, "Stability and capacity of regular wireless networks," *IEEE Trans. Inf. Theory*, vol. 51, no. 6, pp. 1938–1953, Jun. 2005.
[14] F. Baccelli, B. Blaszczyszyn, and P. Muhlethaler, "An Aloha protocol for multihop mobile wireless networks," *IEEE Trans. Inf. Theory*, vol. 52, no. 2, pp. 421–436, Feb. 2006.
[15] R. K. Ganti and M. Haenggi, "Bounds on information propagation delay in interference-limited ALOHA networks," in *Proc. IEEE 7th Int. Symp. Model. Optim. Mobile Ad Hoc Wireless Netw. (WiOpt)*, 2009, pp. 1–7.
[16] P. Jacquet, B. Mans, P. Muhlethaler, and G. Rodolakis, "Opportunistic routing in wireless ad hoc networks: Upper bounds for the packet propagation speed," *IEEE J. Sel. Areas Commun.*, vol. 27, no. 7, pp. 1192–1202, Sep. 2009.
[17] Y. Cong, X. Zhou, and R. Kennedy, "Interference prediction in mobile ad hoc networks with a general mobility model," *IEEE Trans. Wireless Commun.*, vol. 14, no. 8, pp. 4277–4290, Aug. 2015.
[18] R. K. Ganti and M. Haenggi, "Spatial and temporal correlation of the interference in ALOHA ad hoc networks," *IEEE Commun. Lett.*, vol. 13, no. 9, pp. 631–633, Sep. 2009.
[19] Z. Gong and M. Haenggi, "Interference and outage in mobile random networks: Expectation, distribution, and correlation," *IEEE Trans. Mobile Comput.*, vol. 13, no. 2, pp. 337–349, Feb. 2014.
[20] X. Zhang and M. Haenggi, "Random power control in Poisson networks," *IEEE Trans. Commun.*, vol. 60, no. 9, pp. 2602–2611, Sep. 2012.
[21] F. Baccelli and B. Baszczyszyn, "A new phase transition for local delays in MANETs," in *Proc. IEEE INFOCOM*, 2010, pp. 1–9.
[22] M. Haenggi, "The local delay in Poisson networks," *IEEE Trans. Inf. Theory*, vol. 59, no. 3, pp. 1788–1802, Mar. 2013.
[23] J. Zhu, Y. Chen, Y. Shen, O. Takahashi, X. Jiang, and N. Shiratori, "Secrecy transmission capacity in noisy wireless ad hoc networks," *Ad Hoc Netw.*, vol. 21, pp. 123–133, 2014.
[24] X. Zhou, R. K. Ganti, J. G. Andrews, and A. Hjorungnes, "On the throughput cost of physical layer security in decentralized wireless networks," *IEEE Trans. Wireless Commun.*, vol. 10, no. 8, pp. 2764–2775, Aug. 2011.
[25] R. R. Rao and A. Ephremides, "On the stability of interacting queues in a multiple-access system," *IEEE Trans. Inf. Theory*, vol. 34, no. 5, pp. 918–930, Sep. 1988.
[26] A. E. Gamal, J. Mammen, B. Prabhakar, and D. Shah, "Optimal throughput-delay scaling in wireless networks—Part I: The fluid model," *IEEE Trans. Inf. Theory*, vol. 52, no. 6, pp. 2568–2592, Jun. 2006.
[27] W. Hsu, T. Spyropoulos, K. Psounis, and A. Helmy, "Modeling time-variant user mobility in wireless mobile networks," in *Proc. IEEE INFOCOM*, 2007, pp. 758–766.
[28] M. Garetto, P. Giaccone, and E. Leonardi, "Capacity scaling in ad hoc networks with heterogeneous mobile nodes: The subcritical regime," *IEEE/ACM Trans. Netw.*, vol. 17, no. 6, pp. 1888–1901, Dec. 2009.
[29] X. Lin and N. Shroff, "The fundamental capacity-delay tradeoff in large mobile ad hoc networks," in *Proc. 3rd Annu. Mediterr. Ad Hoc Netw. (MedHoc)*, 2004, pp. 1–13.
[30] M. Neely, "Dynamic power allocation and routing for satellite and wireless networks with time varying channels," Ph.D. dissertation, Department of Electrical Engineering and Computer Science, Massachusetts Inst. Technol., Cambridge, MA, USA, 2003.
[31] P. Gupta and P. Kumar, "The capacity of wireless networks," *IEEE Trans. Inf. Theory*, vol. 46, no. 2, pp. 388–404, Mar. 2000.
[32] H. Daduna, *Queueing Networks With Discrete Time Scale: Explicit Expressions for the Steady State Behavior of Discrete Time Stochastic Networks*. New York, NY, USA: Springer, 2001.
[33] F. Baccelli and B. Blaszczyszyn, *Stochastic Geometry and Wireless Networks—Part I: Theory*. Boston, MA, USA: Now Publishers Inc., 2009.
[34] D. J. Daley and D. Vere-Jones, *An Introduction to The Theory of Point Processes*. New York, NY, USA: Springer, 1988.
[35] Y. Chen. (2014). *A C++ Simulator for the ALOHA MANET* [Online]. Available: https://www.researchgate.net/publication/261597416.
[36] P. Nain, D. Towsley, B. Liu, and Z. Liu, "Properties of random direction models," in *Proc. IEEE INFOCOM*, 2005, pp. 1897–1907.
[37] T. Camp, J. Boleng, and V. Davies, "A survey of mobility models for ad hoc network research," *Wireless Commun. Mobile Comput.*, vol. 2, no. 5, pp. 483–502, 2002.
[38] S. Srinivasa and M. Haenggi, "Distance distributions in finite uniformly random networks: Theory and applications," *IEEE Trans. Veh. Technol.*, vol. 59, no. 2, pp. 940–949, Feb. 2010.

Yin Chen (M'14) received the B.S. and M.S. degrees both in computer science from Xidian University, Xi'an, China, in 2008 and 2011, respectively, and the Ph.D. degree in systems information science from Future University Hakodate, Hakodate, Japan, in 2014. He is currently serving as a Research Assistant Professor with Shonan Fujisawa Campus, Keio University, Fujisawa, Japan. From April to October 2014, he was as a Postdoctoral Researcher with Future University Hakodate. His research interests include wireless communication and networks, in particular modeling and performance evaluation of wireless networks based on queuing theory and stochastic geometry.

Yulong Shen (M'09) received the B.S. and M.S. degrees in computer science and the Ph.D. degree in cryptography from Xidian University, Xi'an, China, in 2002, 2005, and 2008, respectively. He is currently an Associate Professor with the School of Computer Science and Technology, Xidian University. He is also an Associate Director of the Shaanxi Key Laboratory of Network and System Security and a Member of the State Key Laboratory of Integrated Services Networks, Xidian University. His research interests include wireless network security. He is an ACM Member. He has also served on the technical program committees of several international conferences, including ICEBE, INCoS, CIS, and SOWN.

Jinxiao Zhu received the B.S. and M.E. degrees in software engineering from Xidian University, Xi'an, China, in 2008 and 2011, respectively, and the Ph.D. degree in systems information science from Future University Hakodate, Hakodate, Japan, in 2014. She is currently a Researcher with National Institute of Information and Communications Technology (NICT), Japan. From April 2014 to January 2015, she was a Postdoctoral Researcher with Future University Hakodate, Hakodate, Japan. Her research interests include information-theoretic security for wireless communications and performance evaluation of wireless networks.

Xiaohong Jiang (M'03–SM'09) received the B.S., M.S., and Ph.D. degrees from Xidian University, Xi'an, China, in 1989, 1992, and 1999, respectively. He is currently a Full Professor with Future University Hakodate, Hakodate, Japan. Before joining Future University Hakodate, he was an Associate Professor with Tohoku University, Sendai, Japan, and an Assistant Professor with the Graduate School of Information Science, Japan Advanced Institute of Science and Technology (JAIST), Nomi, Japan. His research interests include wireless sensor networks, optical networks, and network coding. He has authored and coauthored more than 190 publications in journals, books, and international conference proceedings, which include the IEEE/ACM TRANSACTIONS ON NETWORKING, the IEEE TRANSACTIONS ON COMMUNICATIONS, and the IEEE JOURNAL OF SELECTED AREA ON COMMUNICATIONS. He was the recipient of the Best Paper Award of WCNC'08 and the ICC2005—Optical Networking Symposium.

Hideyuki Tokuda (M'10) obtained the B.S. and M.S. degrees from Keio University, Tokyo, Japan, in 1975 and 1977, respectively, and the Ph.D. degree in computer science from the University of Waterloo, Waterloo, ON, Canada, in 1983. After he completed the Ph.D., he joined the School of Computer Science, Carnegie Mellon University, Pittsburgh, PA, USA, and worked on distributed real-time operating systems such as real-time Mach, and the ARTS Kernel. In 1990, he returned to Keio University and worked on many national R&D projects. His research interests include OS, ubiquitous computing systems, IoT/IoE, cyber-physical systems, and smart cities. He is a Member of Science Council of Japan, the Vice President of IPSJ, an Assistant to NISC, an IPSJ Fellow, an JSSST Fellow, and a Member of ACM, IEICE, and JSSST.